Contribution from the Department of Chemistry,
University of North Carolina, Chapel Hill, North Carolina 27514

Synthesis and Structural and Magnetic Characterization of Bis[dibromo[2-(2-methylaminoethyl)pyridine]copper(II)]

ROXY B. WILSON, WILLIAM E. HATFIELD, and DEREK J. HODGSON*

Received January 22, 1976

AIC600628

The complex bis[dibromo[2-(2-methylaminoethyl)pyridine]copper(II)], $[Cu(C_8H_{12}N_2)Br_2]_2$ or $[Cu(MAEP)Br_2]_2$, has been synthesized, and its crystal structure has been determined from three-dimensional counter x-ray data. The complex crystallizes in the space group $P\bar{1}$ of the triclinic system, with one dimeric formula unit in a cell of dimensions $a = 9.545$ (3) Å, $b = 7.015$ (2) Å, $c = 9.221$ (3) Å, $\alpha = 76.13$ (2)°, $\beta = 76.49$ (2)°, and $\gamma = 102.12$ (3)°. The observed and calculated densities are 2.14 and 2.151 g cm^{-3}, respectively. Least-squares refinement of the structure using 1945 independent intensities has led to a final value of the conventional R factor (on F) of 0.038. The complex consists of pairs of trigonal-bipyramidal copper(II) centers which share a face, the two bridging bromide ions each being equatorial to one copper atom and axial to the other. The trigonal coordination consists of two bromide ligands and the aromatic nitrogen atom, while the axial sites are occupied by the other bridging bromide ion and the aliphatic nitrogen atom. The Cu–Cu separation in the dimer is 3.803 Å, the bridging Cu–Br bond lengths being 2.47 and 2.80 Å. The magnetic susceptibility of a powdered sample of the complex has been measured in the temperature range 2–70 K. The data show a maximum at 4 K and demonstrate exchange coupling with $g = 2.15$ and $2J = -4.3$ cm^{-1}.

Introduction

Uhlig and Maaser first reported the synthesis of compounds of formulation $Cu(AEP)X_2$, where AEP is 2-(2-aminoethyl)pyridine and X is a halide, and postulated that these complexes were dihalogen-bridged dimers with tetragonal-pyramidal geometry at the copper atoms.[1] Structural investigations showed that $Cu(AEP)Cl_2$ and $Cu(AEP)Br_2$ are best described as six-coordinate polymers containing monohalogen bridges connecting dihalogen-bridged dimers. Both types of interactions are weak with apical Cu–Br distances of 3.71 and 3.57 Å and Cu–Cl distances 3.50 and 3.52 Å for the pairwise and chainwise interactions, respectively.[2,3] Because of the two separate pathways for spin–spin interactions, the magnetic properties of these two compounds are difficult to account for accurately.[4]

A similar structural complexity was encountered in the compounds $Cu(py)_2X_2$ (py = pyridine)[5,6] which are six-coordinate polymers. A simplifying change occurs when pyridine is replaced by 2-methylpyridine (α-picoline or pic), and the compounds $Cu(pic)_2X_2$ are five-coordinate dimers.[7,8] Thus we undertook[9] an investigation of $Cu(MAEP)Cl_2$, where MAEP is 2-(2-methylaminoethyl)pyridine, hoping that the presence of the methyl group might inhibit six-coordination by blocking approach to the copper center from one direction. This was the case, but the pairwise interaction was the one eliminated, the structure consisting of tightly bound monochloro-bridged chains with tetragonal-pyramidal geometry at the copper centers. Despite the wide variety of structural types reported for compounds of the formulation $CuLX_2$ (where L is bidentate) or CuA_2X_2 (where A is monodentate),[2,3,5–8,10–16] the structure of $Cu(MAEP)Cl_2$ is only the second of its type for this class of compounds, and investigation of its magnetic properties is currently under way. The structures of a number of halogen-bridged compounds have been investigated in hope of correlating their structural and magnetic properties.[7,8,10,11,17–21] We felt that such an investigation of $Cu(MAEP)Br_2$ would further our understanding of the AEP systems as well as the general class of halogen-bridged compounds. Consequently, we have undertaken a complete structural and magnetic investigation of this complex.

Experimental Section

The complex was prepared by addition of 0.232 g (0.001 mol) of anhydrous $CuBr_2$ to a solution containing 0.150 g (0.001 mol) of ligand in 20 ml of absolute methanol. The resultant dark green solution was warmed with stirring until all $CuBr_2$ was dissolved; dark green crystals precipitated upon overnight refrigeration. Anal. Calcd for $CuBr_2N_2C_8H_{12}$: C, 26.72; H, 3.36; N, 7.79. Found: C, 26.90; H, 3.47; N, 7.73. Weissenberg and precession photographs indicated that the crystals belong to the triclinic system and that the space group is either C_1^1-$P1$ or C_i^1-$P\bar{1}$; the centrosymmetric space group was chosen and this choice was apparently validated by the successful refinement of the structure. The cell constants, obtained by least-squares methods, are $a = 9.545$ (3) Å, $b = 7.015$ (2) Å, $c = 9.221$ (3) Å, $\alpha = 76.13$ (2)°, $\beta = 76.49$ (2)°, and $\gamma = 102.12$ (3)°; the observations were made at 22 °C using Mo Kα_1 radiation with an assumed wavelength of 0.7093 Å. A calculated density of 2.151 g cm^{-3} for two monomeric units in the cell was in good agreement with the observed value of 2.14 g cm^{-3} obtained by flotation in a mixture of bromoform, toluene, and diiodomethane.

Diffraction data were collected from a roughly diamond-shaped plate with faces (100), ($\bar{1}$00), (010), (0$\bar{1}$0), (001), (00$\bar{1}$), (011), and (0$\bar{1}\bar{1}$). The separations between opposite pairs of faces were as follows: (100) and ($\bar{1}$00), 0.040 cm; (010) and (0$\bar{1}$0), 0.025 cm; (001) and (00$\bar{1}$), 0.008 cm; (011) and (0$\bar{1}\bar{1}$), 0.022 cm. The crystal was mounted roughly perpendicular to the (100) face, and intensity data were collected on a Picker four-circle automatic diffractometer equipped with a graphite monochromator using Mo Kα radiation at a takeoff angle of 1.2°. The receiving aperture was 5.0 × 5.0 mm and was placed 32 cm from the crystal. Data were collected in the θ–2θ scan mode at a rate of 1°/min; peaks were scanned from 0.50° below the calculated Mo Kα_1 peak position to 0.50° above the calculated Mo Kα_2 peak position. Stationary-counter, stationary-crystal backgrounds of 10 s were collected at both ends of each scan. The pulse height analyzer was set for an approximately 90% window centered on the Mo Kα peak.

A single form of the data ($\pm h,-k,\pm l$) was collected out to a 2θ value (Mo Kα) of 55°, above which there were few intensities greater than background. A total of 2619 reflections were recorded, including several Friedel pairs in the event the space group proved to be noncentrosymmetric. Three standard reflections were examined following each 100 reflections and their intensities showed no systematic decline as a function of exposure time. The data were processed using the method of Ibers and co-workers[22] and their formula $\sigma(I) = [C + 0.25(t_s/t_b)^2(B_H + B_L) + p^2I^2]^{1/2}$ for the estimated standard deviation, the value of p being assigned[23] as 0.03. The values of I and $\sigma(I)$ were corrected for Lorentz–polarization effects using the expression[24]

$$\frac{1}{Lp} = \frac{2 \sin 2\theta}{\cos^2 2\theta_m + \cos^2 2\theta}$$

where the angle of the monochromator, θ_m, was 12°, and for absorption. The attenuation coefficient for Mo Kα radiation was 95.47 cm^{-1}, and the transmission coefficients ranged from 0.11 to 0.48. Of the 2619 data collected, 2115 had intensities greater than 3 times their estimated standard deviation; 1945 of these were independent.

Table I. Positional Parameters[a] for $[Cu(MAEP)Br_2]_2$

Atom	x	y	z
Cu(1)	1616 (1)	−93 (1)	3386 (1)
Br(1)	2153 (1)	2351 (1)	867 (1)
Br(2)	1315 (1)	2419 (1)	4821 (1)
N(1)	2652 (5)	−1505 (6)	4852 (5)
N(2)	1718 (5)	−2430 (6)	2466 (5)
C(2)	3933 (5)	−1862 (7)	4144 (6)
C(3)	4769 (6)	−2733 (8)	5003 (8)
C(4)	4232 (7)	−3345 (8)	6615 (8)
C(5)	2899 (8)	−3054 (9)	7338 (8)
C(6)	2141 (7)	−2105 (8)	6416 (6)
C(7)	4398 (6)	−1228 (8)	2390 (7)
C(8)	3280 (6)	−2349 (8)	1711 (7)
C(9)	745 (9)	−2805 (10)	1466 (8)
H(3)	574 (6)	−286 (7)	441 (6)
H(4)	487 (8)	−391 (10)	725 (8)
H(5)	252 (7)	−344 (9)	816 (7)
H(6)	140 (8)	−201 (10)	697 (9)
H(7)	457 (6)	31 (7)	204 (6)
H(7)′	544 (9)	−131 (10)	183 (9)
H(8)	332 (6)	−366 (9)	176 (6)
H(8)′	362 (6)	−148 (8)	68 (7)
H(9)	−6 (9)	−296 (11)	188 (9)
H(9)′	77 (6)	−417 (8)	122 (7)
H(9)″	98 (9)	−176 (12)	42 (10)
H(N)	133 (9)	−332 (11)	358 (9)

[a] Positional parameters for nonhydrogen atoms are $\times 10^4$; those for hydrogen atoms are $\times 10^3$.

Solution and Refinement of Structure

A three-dimensional Patterson function[25] yielded the positions of the copper and two bromine atoms, and two cycles of least-squares refinement on these positions were carried out. All least-squares refinements in this analysis were carried out on F, with minimization of the function $\sum w(|F_o| - |F_c|)^2$ where the weight w is taken as $4F_o^2/\sigma^2(F_o^2)$. In calculation of F_c, the atomic scattering factors for Cu, Br, and N were those calculated by Cromer and Waber,[26] those for C were calculated by Ibers,[27] and those for H were calculated by Stewart, Davidson, and Simpson.[28] Anomalous dispersion of Cu and Br was also included in the calculation of F_c, the values of $\Delta f'$ and $\Delta f''$ being those computed by Cromer and Liberman.[29] The remaining ten nonhydrogen atoms were located from a difference Fourier synthesis and isotropic least-squares refinement of these positions yielded values of the conventional residuals $R_1 = \sum(|F_o| - |F_c|)/\sum|F_o|$ and $R_2 = [\sum w(|F_o| - |F_c|)^2/\sum w(F_o)^2]^{1/2}$ of 0.125 and 0.166, respectively. Anisotropic refinement of these atoms gave $R_1 = 0.051$ and $R_2 = 0.077$. At this point an attempt was made to locate hydrogen atoms from the subsequent difference Fourier synthesis, but because of residual electron density around the bromine positions, the positions of the hydrogen atoms were obscured. Therefore, the hydrogen atoms were placed in calculated positions and allowed to vary isotropically, yielding $R_1 = 0.038$ and $R_2 = 0.046$. Examination of $|F_o|$ and $|F_c|$ for the strong low-order data suggested that no correction for secondary extinction was necessary.

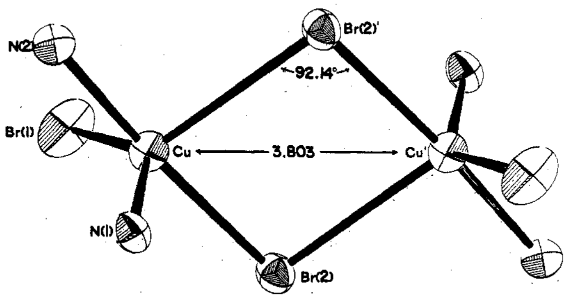

Figure 1. View of the dimeric unit in $[Cu(MAEP)Br_2]_2$. Hydrogen atoms are omitted for clarity.

In the final cycle of least-squares refinement, no atom parameter changed more than 0.67 times its estimated standard deviation, indicating that refinement had converged. The value of R_2 showed no abnormal dependence on $|F_o|$ or $\sin\theta$, showing that our weighting scheme was correct. The final difference Fourier map continued to show residual electron density around the bromine and copper positions, but no peak other than these was higher than 0.51 e Å^{-3}. The positional and thermal parameters are presented in Tables I and II; a compilation of observed and calculated structure amplitudes is available.[30]

Description of the Structure

The structure consists of dimeric $[Cu(MAEP)Br_2]_2$ units as shown in Figure 1. The Cu–Br(2)–Cu′–Br(2)′ bridging unit is strictly planar, owing to the presence of a crystallographic inversion center in the middle of the dimer. The geometry around each copper atom is approximately trigonal bipyramidal, the equatorial (in plane) atoms being two bromine atoms (one terminal and one bridging) and the pyridine nitrogen atom from the MAEP ligand. The axial sites are occupied by the aliphatic nitrogen atom of the MAEP ligand and Br(2)′, which also occupies an equatorial site on the adjacent copper atom. A view of the coordination about one copper atom is shown in Figure 2.

The Cu atom and the three equatorial atoms are nearly coplanar, their deviations from the best least-squares being 0.05 Å or less. Of the three other possible planes which contain copper and three of the five coordinated atoms, only the Cu–Br(2)–N(1)–N(2) plane contains an atom which deviates more than 0.05 Å from the calculated best least-squares plane; Cu lies 0.08 Å out of this plane.

Table II. Thermal Parameters (A^2) for $[Cu(MAEP)Br_2]_2$[a]

Atom	U_{11}	U_{22}	U_{33}	U_{12}	U_{13}	U_{23}
Cu(1)	364 (4)	298 (3)	299 (3)	151 (2)	−121 (3)	−66 (2)
Br(1)	970 (6)	353 (3)	356 (3)	246 (3)	−209 (3)	−19 (2)
Br(2)	295 (3)	309 (2)	405 (3)	99 (2)	−89 (2)	−111 (2)
N(1)	301 (21)	283 (18)	349 (22)	100 (16)	−114 (18)	−59 (16)
N(2)	349 (24)	300 (19)	312 (21)	87 (17)	−93 (18)	−51 (16)
C(2)	271 (26)	246 (21)	407 (28)	88 (19)	−101 (22)	−77 (19)
C(3)	306 (29)	363 (26)	640 (39)	157 (23)	−209 (28)	−200 (26)
C(4)	556 (39)	363 (27)	665 (41)	243 (27)	−414 (34)	−176 (27)
C(5)	527 (40)	405 (29)	356 (33)	110 (26)	−195 (30)	−19 (25)
C(6)	320 (30)	388 (26)	331 (28)	88 (22)	−135 (24)	−73 (22)
C(7)	267 (27)	388 (27)	416 (30)	81 (22)	−23 (24)	−96 (23)
C(8)	342 (30)	363 (27)	343 (28)	91 (22)	−1 (23)	−116 (22)
C(9)	465 (41)	515 (35)	452 (37)	85 (29)	−182 (32)	−217 (29)

Atom	U	Atom	U	Atom	U
H(3)	3 (1)	H(7)	3 (1)	H(9)	7 (3)
H(4)	6 (2)	H(7)′	7 (2)	H(9)′	4 (1)
H(5)	3 (2)	H(8)	3 (1)	H(9)″	8 (3)
H(6)	5 (2)	H(8)′	4 (1)	H(N)	7 (2)

[a] Anisotropic parameters are $\times 10^4$; isotropic, $\times 10^2$. The form of the anisotropic thermal ellipsoid is $\exp[-2\pi^2(U_{11}h^2a^{*2} + U_{22}k^2b^{*2} + U_{33}l^2c^{*2} + 2U_{12}hka^*b^* + 2U_{13}hla^*c^* + 2U_{23}klb^*c^*)]$.

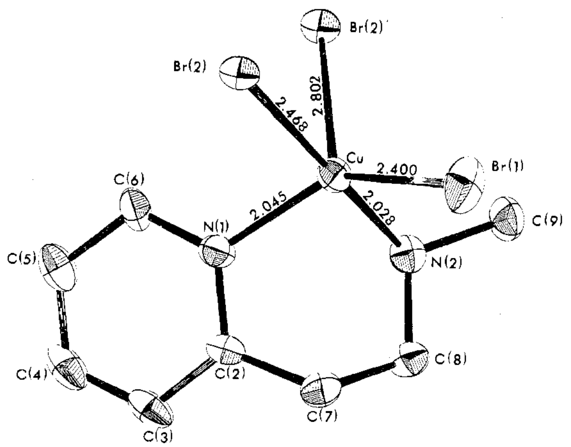

Figure 2. View of the coordination around a single copper(II) center in $[Cu(MAEP)Br_2]_2$. The bridge to the adjacent copper atom is formed by atoms Br(2) and Br(2)′.

Table III. Interatomic Distances (Å) in $Cu(MAEP)Br_2$

Cu–Cu′	3.803 (4)	C(8)–N(2)	1.474 (7)
Cu–Br(1)	2.400 (3)	N(2)–C(9)	1.482 (8)
Cu–Br(2)	2.468 (2)	C(3)–H(3)	1.00 (5)
Cu–Br(2)′	2.802 (4)	C(4)–H(4)	1.01 (7)
Cu–N(1)	2.045 (4)	C(5)–H(5)	0.72 (6)
Cu–N(2)	2.028 (4)	C(6)–H(6)	0.79 (7)
N(1)–C(2)	1.348 (6)	C(7)–H(7)	1.01 (5)
C(2)–C(3)	1.381 (7)	C(7)–H(7)	1.03 (8)
C(3)–C(4)	1.380 (9)	C(8)–H(8)	0.92 (5)
C(4)–C(5)	1.372 (10)	C(8)–H(8)	0.93 (6)
C(5)–C(6)	1.382 (8)	C(9)–H(9)	0.74 (8)
C(6)–N(1)	1.337 (7)	C(9)–H(9)′	1.04 (5)
C(2)–C(7)	1.500 (8)	C(9)–H(9)′	1.01 (8)
C(7)–C(8)	1.532 (8)	N(2)–H(N)	1.00 (8)

Table IV. Interatomic Angles (deg) in $Cu(MAEP)Br_2$

Cu–Br(2)–Cu′	92.14 (9)	Cu–N(2)–C(8)	111.7 (3)
Br(2)–Cu–Br(2)′	87.86 (9)	Cu–N(2)–C(9)	117.5 (4)
Br(2)–Cu–Br(1)	93.95 (8)	N(1)–C(2)–C(3)	121.1 (5)
Br(2)–Cu–N(1)	92.2 (1)	C(2)–C(3)–C(4)	118.9 (5)
Br(2)–Cu–N(2)	172.8 (2)	C(3)–C(4)–C(5)	120.0 (5)
Br(1)–Cu–N(1)	141.6 (1)	C(4)–C(5)–C(6)	118.5 (6)
Br(1)–Cu–N(2)	92.8 (1)	C(5)–C(6)–N(1)	122.0 (6)
Br(1)–Cu–Br(2)′	122.21 (9)	C(6)–N(1)–C(2)	119.4 (4)
N(1)–Cu–N(2)	83.9 (2)	N(1)–C(2)–C(7)	116.3 (4)
N(1)–Cu–Br(2)′	95.8 (1)	C(3)–C(2)–C(7)	122.6 (5)
N(2)–Cu–Br(2)′	86.5 (1)	C(2)–C(7)–C(8)	114.1 (4)
Cu–N(1)–C(2)	115.5 (3)	C(7)–C(8)–N(2)	112.5 (4)
Cu–N(1)–C(6)	125.0 (4)	C(8)–N(2)–C(9)	111.6 (5)

The relevant interatomic distances and angles are given in Tables III and IV. The terminal Cu–Br distance of 2.400 Å is within the range of values 2.34–2.79 Å reported for monomeric and dimeric complexes with terminal Br ligands.[8,31–36] The bridging axial and equatorial Cu–Br(2) and Cu–Br(2)′ distances of 2.47 and 2.80 Å are, as expected, longer than the terminal Cu–Br(1) distance. Bromine-bridged copper dimers and polymers typically show one long and one short bridging Cu–Br distance, as does $[Cu(MAEP)Br_2]_2$. However, the Cu–Br(2) distance is longer than the previously reported short distances and the Cu–Br(2)′ distance is shorter than the previously reported long distances.[2,5,8,34] Thus, in this complex the two Cu–Br bonds are more symmetric than in the others. The weak Cu–Br(2)′ interaction is equatorial rather than axial; this is also the case for other trigonal-bipyramidal dimers.[17–19] The Cu–N separations of 2.028 and 2.045 Å are normal, with the distance to the aliphatic nitrogen atom longer than that to the aromatic nitrogen atom.

The geometry of the MAEP ligand may be compared to that of other substituted aminoethylpyridines in metal complexes.[2,3,9,31,37–42] As in all of these complexes, the atoms in the chelate ring retain the rigid-boat conformation. The base of the boat formed by N(1), N(2), C(2), and C(8) is approximately planar with a mean deviation of 0.07 Å from the best least-squares plane, while Cu and C(7) are 1.21 and 0.60 Å above the plane. It has been noted[9] that when the chelating angle [the N(1)–Cu–N(2) angle] is acute, the copper atom is further from the plane, and when this angle is obtuse, C(7) is further from the plane. This correlation appears to hold true for $[Cu(MAEP)Br_2]_2$ whose chelating angle is 83.9°, even though both nitrogen atoms are not in the equatorial plane of the metal as is the case for all previous complexes of substituted aminoethylpyridines. The pyridine ring is roughly planar, with no atom deviating more than 0.021 Å from the best least-squares plane. The interatomic distances and angles in the pyridine ring and extracyclic portion of the ligand are in the normal ranges.[9,37–43]

There is no evidence for hydrogen bonding in the complex. The only well-documented N–H---Br hydrogen bonding occurs in various forms of ammonium bromide, which has H---Br and Br---N separations of 2.43 and 3.45 Å, respectively.[43–46] In $[Cu(MAEP)Br_2]_2$ there is an H---Br separation of 2.93 Å, but the associated N---Br separation of 3.76 Å is 0.30 Å greater than the sum of the van der Waals radii of nitrogen and bromine.[47] Also, the N(2)–HN---Br(2) angle of 128° indicates that there is probably no hydrogen-bond formation.[48] Other long-range interactions could include interdimer Cu–Br or Br–Br contacts. The shortest of these is a Br(2)–Br(2) separation of 4.85 Å, almost 1 Å longer than twice the van der Waals radius of bromine.[47] We conclude that only extremely weak, if any, long-range interactions are present in this complex.

The trigonal-bipyramidal geometry of $[Cu(MAEP)Br_2]_2$ is unique for bromine-bridged dimers and polymers of copper, since all previously reported structures known to us have either pseudooctahedral or square-pyramidal geometry at the copper centers.[8,14,25,34,49] Since the geometry around copper is not tetragonal pyramidal, the position of the sixth coordination site is more difficult to determine. The C(9) methyl group lies between Br(1) and Br(2)′ (see Figure 2) blocking approach from this direction. However, the N(1)–Cu–Br(1) angle of 141.6° is much more distorted than the Br(1)–Cu–Br(2)′ angle of 122.2°, which suggests that the most likely approach for a sixth ligand is between N(1) and Br(1). Approach in this direction is blocked by H(7); a similar impediment is found in $[Cu(MAEP)Cl_2]_x$.[9] It is tempting to assume that $[Cu(MAEP)Br_2]_2$ takes the form of a trigonal bipyramid because of the steric interaction of two cis bromine ligands at an angle of 90°. However, such a configuration obtains for $[Cu(tmen)Br]_2$ (tmen = *N,N,N′,N′*-tetramethylethylenediamine),[34] which is tetragonal pyramidal, and it is not clear why the trigonal-bipyramidal configuration is adopted in the present case.

Comparison can be made between the present compound and the dichloro-bridged trigonal-bipyramidal dimers $[Cu(guan)Cl_3]_2 \cdot 2H_2O$ (guan = guaninium) and $[CuCl_4]_2^{4-}$, if the 0.15 Å larger covalent radius of bromine[47] is taken into account. The two copper to bridging bromine separations in $[Cu(MAEP)Br_2]_2$ are intermediate between the analogous adjusted Cu–Cl separations of the other compounds. However, the Cu–Br(2)–Cu′ bridge angle of 92.1° is much smaller than the Cu–Cl–Cu′ angles of the other two complexes. Thus, no simple prediction can be made as to the magnitude of the exchange interaction in this complex relative those in the other known trigonal-bipyramidal chlorine-bridged dimers.

Magnetic Properties

The magnetic susceptibility of a powdered sample of $[Cu[MAEP]Br_2]_2$, prepared by pulverizing a crystalline sample, was measured on a Foner-type vibrating-sample

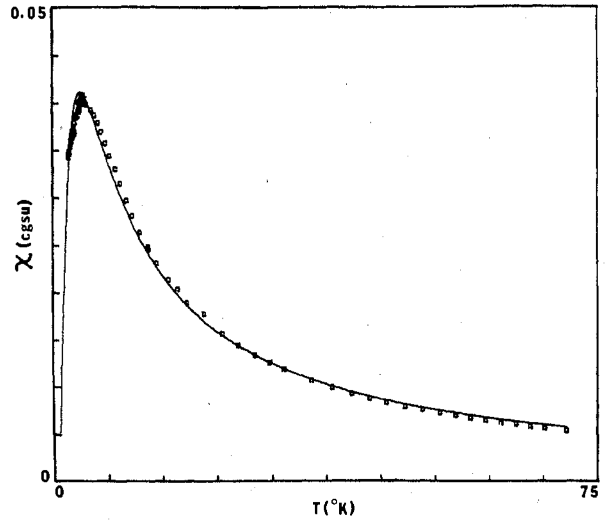

Figure 3. Temperature variation of the magnetic susceptibility (per copper atom) of $[Cu(MAEP)Br_2]_2$. The observed data are shown as squares. The solid line represents the fit to eq 1 (see text), with $2J = -4.3\ cm^{-1}$, $g = 2.15$, and $\gamma = -3.41$.

magnetometer[50] over the temperature range of 2–70 K. Temperatures were measured by a gallium arsenide diode, using tetrathiocyanatocobaltate(II) as a susceptibility standard.[51]

The temperature variation of the magnetic susceptibility is shown in Figure 3, the maximum occurring at approximately 4 K. Since the singlet–triplet splitting, $2J$, was expected to be on the order of gBH and the Bleaney–Bowers equation[52]

$$\chi_m = \frac{Ng^2\beta^2}{3k(T-\Theta)}[1 + {}^1/_3 \exp(-2J/kT)]^{-1}$$

assumes $2J >>> gBH$, this was deemed an inappropriate model for our compound.[53] Using a least-squares technique, the data were fit to the magnetization expression[54]

$$M = \frac{Ng \sinh (g\beta H/kT)}{\exp(-2J/kT) + 2 \cosh (g\beta H/kT) + 1} \qquad (1)$$

which yielded values of $g = 1.87$ and $2J = -4.1\ cm^{-1}$. An attempt was made to improve agreement by taking into account weak interpair exchange using the method of Friedberg and co-workers.[54] Utilizing the relationship $H = H_0 + \gamma M$ where H is the effective field and H_0 is the external field, eq 1 becomes a self-consistent equation which can be solved by repeated interaction. The best least-squares fit to this expression minimizing the function $F = \sum_i[(M(\text{obsd})_i - M(\text{calcd})_i)T_i]^2$ yields a more reasonable g value of 2.15 with $2J = -4.3\ cm^{-1}$ and $\gamma = -3.41$ and gives a much better fit to the observed data. Using the equation $J' = \gamma Ng^2\beta^2k/2Z$ where Z is the number of nearest neighbors (in this case 4),[55] a value of $-0.51\ cm^{-1}$ is obtained for the lattice interaction parameter J'. Although small values of J' have been observed for other copper dimers,[53,56] $-0.51\ cm^{-1}$ seems unusually large in view of the absence of long-range interactions in the complex (vide supra). It is noteworthy that a similar coupling constant has been observed in $[Cu_2Br_6]^{2-}$, where the interdimer separations are also large.[57]

As is the case for out-of-plane dimers (one bridging atom apical and one equatorial to the metal atom),[8,53,58,59] the magnitude of the exchange interaction is small for $[Cu(MAEP)Br_2]_2$. The Cu–Br–Cu angle of 92.1° is smaller than the bridge angle in $[Cu_2Cl_8]^{4-}$ or $[Cu(guan)Cl_3]_2$ as is the magnitude of $2J$, but there is not a linear relationship between the two. It has been noted[59] that there are both bond length and bond angle effects in dimers of this type. Although the Cu–Br distances are longer in this compound than the adjusted Cu–Cl separations in $[Cu(guan)Cl_3]_2$, they are very similar to those in $[Cu_2Cl_8]^{4-}$. Thus, for compounds with similar copper–halogen separations, a decrease in bond angle is accompanied by a decrease in $|2J|$. Investigations of other halogen-bridged copper dimers are under way so that we may further understand the twofold effect of bridge geometry on magnetic exchange.

Acknowledgment. We are grateful to Mr. W. E. Estes for assistance in obtaining the magnetic data and to Mr. R. P. Scaringe for assistance in fitting them to the theoretical models. This research was supported by Grant MPS73-08703 A02 from the National Science Foundation.

Registry No. $[Cu(MAEP)Br_2]_2$, 59109-90-9.

Supplementary Material Available: Listing of structure factor amplitudes (11 pages). Ordering information is given on any current masthead page.

References and Notes

(1) E. Uhlig and M. Maaser, *Z. Anorg. Allg. Chem.*, **322**, 25 (1963).
(2) V. C. Copeland, P. Singh, W. E. Hatfield, and D. J. Hodgson, *Inorg. Chem.*, **11**, 1826 (1972).
(3) V. C. Copeland, W. E. Hatfield, and D. J. Hodgson, *Inorg. Chem.*, **12**, 1340 (1973).
(4) D. Y. Jeter, W. E. Hatfield, and D. J. Hodgson, *J. Phys. Chem.*, **76**, 2707 (1972).
(5) (a) J. D. Dunitz, *Acta Crystallogr.*, **10**, 307 (1957); (b) V. Kupcik and S. Durovic, *Czech. J. Phys. (Engl. Trans.)*, **10**, 182 (1960); (c) B. Morosin, *Acta Crystallogr., Sect. B*, **31**, 632 (1975).
(6) R. D. Willett and K. Chang, *Inorg. Chim. Acta*, **4**, 447 (1970).
(7) V. F. Duckworth and N. C. Stephenson, *Acta Crystallogr., Sect. B*, **25**, 1795 (1969).
(8) P. Singh, D. Y. Jeter, W. E. Hatfield, and D. J. Hodgson, *Inorg. Chem.*, **11**, 1657 (1972).
(9) R. A. Bream, E. D. Estes, and D. J. Hodgson, *Inorg. Chem.*, **14**, 1672 (1975).
(10) D. H. Svedung, *Acta Chem. Scand.*, **23**, 2865 (1969).
(11) E. D. Estes, W. E. Hatfield, and D. J. Hodgson, *Inorg. Chem.*, **14**, 106 (1975).
(12) W. Stahlin and H. R. Oswald, *Acta Crystallogr., Sect. B*, **27**, 1368 (1971).
(13) E. D. Estes and D. J. Hodgson, *J. Chem. Soc., Dalton Trans.*, 1168 (1975).
(14) F. Hanic, *Acta Crystallogr.*, **12**, 739 (1959).
(15) M. Laing and E. Horsfield, *Chem. Commun.*, 735 (1968).
(16) M. Laing and G. Carr, *J. Chem. Soc. A*, 1141 (1971).
(17) D. J. Hodgson, P. K. Hale, and W. E. Hatfield, *Inorg. Chem.*, **10**, 1061 (1971).
(18) J. P. DeClerq, M. Debbaudt, and M. van Meersche, *Bull. Soc. Chim. Belg.*, **80**, 527 (1971).
(19) M. Sundaralingam and J. A. Carrabine, *J. Mol. Biol.*, **60**, 287 (1971).
(20) R. D. Willett and C. Chow, *Acta Crystallogr., Sect. B*, **30**, 207 (1974).
(21) M. Textor, E. Dubler, and H. R. Oswald, *Inorg. Chem.*, **13**, 1361 (1974).
(22) P. W. R. Corfield, R. J. Doedens, and J. A. Ibers, *Inorg. Chem.*, **6**, 197 (1967).
(23) W. R. Busing and H. A. Levy, *J. Chem. Phys.*, **26**, 563 (1967).
(24) S. A. Goldfield and K. N. Raymond, *Inorg. Chem.*, **10**, 2604 (1971).
(25) For a description of the programs used in this solution and refinement see ref 8.
(26) D. T. Cromer and J. T. Waber, *Acta Crystallogr.*, **18**, 104 (1965).
(27) J. A. Ibers, "International Tabers for X-Ray Crystallography", Vol. III, Kynoch Press, Birmingham, England, 1962, Table 3.3.1A.
(28) R. F. Stewart, E. R. Davidson, and W. T. Simpson, *J. Chem. Phys.*, **42**, 3175 (1965).
(29) D. T. Cromer and D. Liberman, *J. Chem. Phys.*, **53**, 1891 (1970).
(30) Supplementary material.
(31) P. Singh, V. C. Copeland, W. E. Hatfield, and D. J. Hodgson, *J. Phys. Chem.*, **76**, 2887 (1972).
(32) E. D. Estes and D. J. Hodgson, *Inorg. Chem.*, **14**, 334 (1975).
(33) R. Mergehenn and W. Haase, *Acta Crystallogr., Sect. B*, **31**, 1847 (1975).
(34) E. Luukonen and A. Pajunen, *Suom. Kemistil. B*, **46**, 292 (1973).
(35) A. Pajunen and M. Lehtonen, *Suom. Kemistil. B*, **44**, 200 (1971).
(36) W. Haase, *Chem. Ber.*, **106**, 3132 (1973).
(37) V. C. Copeland and D. J. Hodgson, *Inorg. Chem.*, **12**, 2157 (1973).
(38) D. L. Lewis and D. J. Hodgson, *Inorg. Chem.*, **12**, 2935 (1973).
(39) D. L. Lewis and D. J. Hodgson, *Inorg. Chem.*, **13**, 143 (1974).
(40) D. L. Lewis, K. T. McGregor, W. E. Hatfield, and D. J. Hodgson, *Inorg. Chem.*, **13**, 1013 (1974).
(41) D. L. Kozlowski and D. J. Hodgson, *J. Chem. Soc., Dalton Trans.*, 55 (1975).
(42) D. L. Lewis, W. E. Hatfield, and D. J. Hodgson, *Inorg. Chem.*, **11**, 2216 (1972).
(43) A. Smits and D. Tollenaer, *Z. Phys. Chem., Abt. B*, **52**, 222 (1942).
(44) H. A. Levy and S. W. Peterson, *J. Am. Chem. Soc.*, **75**, 1536 (1953).
(45) H. S. Gutowsky, G. B. Kistiakowsky, G. E. Pake, and E. M. Purcell, *J. Chem. Phys.*, **17**, 972 (1949).

(46) G. Bartlet and I. Langmuir, *J. Am. Chem. Soc.*, **43**, 84 (1921).
(47) L. Pauling, "The Nature of the Chemical Bond", 3d ed, Cornell University Press, Ithaca, N.Y., 1960.
(48) W. C. Hamilton and J. A. Ibers, "Hydrogen Bonding in Solids", W. A. Benjamin, New York, N.Y., 1968.
(49) L. Helmholz, *J. Am. Chem. Soc.*, **69**, 886 (1947).
(50) S. Foner, *Rev. Sci. Instrum.*, **30**, 548 (1959).
(51) B. N. Figgis and R. S. Nyholm, *J. Chem. Soc.*, 4190 (1958).
(52) B. Bleaney and K. Bowers, *Proc. R. Soc. London, Ser. A*, **214**, 451 (1952).
(53) E. D. Estes, W. E. Estes, R. P. Scaringe, W. E. Hatfield, and D. J. Hodgson, *Inorg. Chem.*, **14**, 2564 (1975).
(54) B. E. Myers, L. Berger, and S. A. Friedberg, *J. Appl. Phys.*, **40**, 1149 (1969).
(55) J. S. Smart, "Effective Field Theories of Magnetism", W. B. Saunders, Philadelphia, Pa., 1966.
(56) K. T. McGregor, D. J. Hodgson, and W. E. Hatfield, *Inorg. Chem.*, **12**, 731 (1973).
(57) C. Chow, R. D. Willett, and B. C. Gerstein, *Inorg. Chem.*, **14**, 205 (1975).
(58) R. F. Drake, V. H. Crawford, N. W. Laney, and W. E. Hatfield, *Inorg. Chem.*, **13**, 1246 (1974).
(59) K. T. McGregor, D. B. Losee, D. J. Hodgson, and W. E. Hatfield, *Inorg. Chem.*, **13**, 756 (1974).

Notes

Contribution from the Department of Chemistry, Mississippi State University, Mississippi State, Mississippi 39762

Substitution Reactions of Five-Coordinate Complex Ions. 1. Kinetics of Thiocyanate and Cyanide Substitution in a Five-Coordinate Nickel(II) Complex in Methanol

Eugene Grimley,* Jo M. Grimley, Tsong-Dsu Li, and Dwight Emerich

Received May 7, 1975 AIC50313X

Extensive mechanistic studies of ligand substitution reactions in solution have been reported for four-coordinate and six-coordinate transition metal complexes.[1,2] Few studies can be found in the chemical literature concerning ligand substitution of five-coordinate transition metal complexes. Our interest in the kinetics of substitution in five-coordinate complexes stems from an attempt to correlate kinetic data with differences in electronic environment imposed on the metals resulting from donor effects of group 5 and 6 elements.

Pearson, Muir, and Venanzi[3] reported results of an investigation of ligand substitution in a series of five-coordinate platinum(II) and palladium(II) complexes containing the tetradentate ligand tris(*o*-diphenylarsinophenyl)arsine, in methanol. Morgan and Tobe[4] reported kinetics of a study with platinum(II) and palladium(II) complexes containing the tetradentate ligand tris(*o*-dimethylarsinophenyl)arsine, in methanol. We report here the results of an investigation of ligand substitution in a nickel(II) complex in methanol solution that is isostructural[5] with the platinum(II) and palladium(II) complexes previously reported.

Experimental Section

Chemicals. Sodium thiocyanate and the starting material for tris(*o*-diphenylarsinophenyl)arsine, *o*-bromoaniline, were obtained from Eastman Organic Chemicals. Ultrapure nickel(II) chloride tetrahydrate and nickel(II) perchlorate hexahydrate were obtained from Alfa Inorganics, Inc. Dichloromethane and methanol used were Spectroquality grade obtained from Matheson Coleman and Bell. All other chemicals used were reagent grade.

Synthesis and Analysis of QAS. Tris(*o*-diphenylarsinophenyl)arsine, QAS, was prepared[6] as previously reported starting with *o*-bromoaniline. White crystalline material obtained after recrystallization from dichloromethane was found to melt at 241 °C. The reported melting point was 240 °C. Anal.[7] Calcd for $C_{54}H_{42}As_4$: C, 65.45; H, 4.28; As, 30.26. Found: C, 66.00; H, 4.20; As, 29.70.

Synthesis and Analysis of [NiCl(QAS)]ClO$_4$. The complex chlorotris(*o*-diphenylarsinophenyl)arsinenickel(II) perchlorate was prepared as reported by Dyer, Hartley, and Venanzi.[5] To 0.10 g of $NiCl_2 \cdot 4H_2O$ (0.50 mmol) and 0.18 g of $Ni(ClO_4)_2 \cdot 6H_2O$ (0.50 mmol) in a three-neck flask fitted with stirring bar, funnel, and reflux condenser was added 5 ml of ethanol. A pale green solution formed upon stirring to which 0.99 g of QAS (1.0 mmol) was added followed by addition of 20 ml of dichloromethane. After 15 min of refluxing, 20 ml of ethanol was added. The dichloromethane was stripped off, and the flask contents were cooled to 0 °C for several hours, filtered, and washed with cold ethanol yielding 1.09 g (92%) of dark blue crystals. The product decomposed at 321 °C in agreement with a literature value of 321–322 °C. Anal.[7] Calcd for $NiC_{54}H_{42}As_4Cl_2O_4$: Ni, 4.96; C, 54.77; H, 3.57; As, 25.30; Cl, 5.99; O, 5.40. Found: Ni, 4.88; C, 54.50; H, 3.65; As, 23.89; Cl, 6.10; O, not determined.

The ultraviolet–visible spectrum of the complex in dichloromethane solution was obtained. Positions of the absorptions bands (319, 459, and 617 nm) were in agreement with literature values.

Synthesis and Analysis of [Ni(NCS)(QAS)]ClO$_4$. Isothiocyanatotris(*o*-diphenylarsinophenyl)arsinenickel(II) perchlorate was prepared as previously reported.[5] To 0.20 g of $Ni(NO_3)_2 \cdot 6H_2O$ (0.69 mmol) in 5 ml of ethanol was added a solution of 0.11 g of sodium thiocyanate (1.4 mmol) in 5 ml of ethanol. The solution was filtered into a solution of 0.50 g of QAS (0.50 mmol) in 10 ml of dichloromethane and refluxed for 15 min. This solution was then filtered into a solution of 0.50 g of sodium perchlorate monohydrate (3.6 mmol) and the dichloromethane was stripped off by partial vacuum. Resulting black crystals were filtered and dried in a vacuum oven yielding 0.54 g (89%). Agreement with the literature was obtained for the decomposition point and for the positions of absorption bands for dichloromethane solutions of the complex in the ultraviolet and visible spectral range (316, 446, and 585 nm).

Synthesis and Analysis of [Ni(CN)(QAS)]ClO$_4$. A solution of 0.013 g of NaCN (0.27 mmol) in 20 ml of ethanol was added dropwise to a solution of 0.33 g of [NiI(QAS)]ClO$_4$ (0.26 mmol) in 20 ml of warm dichloromethane. The dichloromethane was removed by boiling the mixture. The brown complex obtained was dried in the vacuum oven. The decomposition point was 338–339 °C. Ultraviolet and visible spectra and the decomposition temperature were in agreement with literature values (maximum absorbtion bands: 259, 292, and 465 nm).

Kinetic Measurements and Data Analysis. The wavelengths of greatest difference in molar absorptivity between $[NiCl(QAS)]^+$ and $[Ni(NCS)(QAS)]^+$ in CH_3OH and $[NiCl(QAS)]^+$ and $[Ni(CN)(QAS)]^+$ in CH_3OH were found to be 585 and 465 nm, respectively. Solutions of these complexes in methanol appeared to obey Beer's law at the above wavelengths. Visible spectra taken of reaction mixtures after completion of several reactions indicated that the expected substitution products were obtained and were formed in a nearly 1:1 stoichiometric ratio.

A Beckman DU spectrophotometer fitted with a thermostatically controlled variable-temperature compartment and a rapid-mixing syringe[8] and a Durrum stopped-flow spectrophotometer were used to obtain kinetic data. Reactions were initiated by mixing the appropriate freshly prepared solutions with the temperature being held at 25 ± 0.2 °C. Concentrations of entering ligands were kept in large excess of complex concentrations so that the reaction data were pseudo first order.

Kinetic data gave straight-line plots using the standard integrated first-order rate expression

$$\ln (A_t - A_\infty) = -k_{\text{obsd}}t + \ln (A_0 - A_\infty) \qquad (1)$$

where A is absorbance. The average deviation of the kinetic data was approximately 5% for replicate experiments.

Results and Discussion

The tetradendate structure of tris(*o*-diphenylarsinophenyl)arsine, QAS, and the tripod arrangement of QAS in coordination of nickel(II) to form trigonal-bipyramidal complexes are shown in Figure 1. The stoichiometry representing the net substitution process of [NiCl(QAS)]ClO$_4$